Amino Acids (2012) 43:1189–1202
DOI 10.1007/s00726-011-1174-x

ORIGINAL ARTICLE

Plant aminoaldehyde dehydrogenases oxidize a wide range of nitrogenous heterocyclic aldehydes

Jan Frömmel · Miroslav Soural · Martina Tylichová · David Kopečný · Gabriel Demo · Michaela Wimmerová · Marek Šebela

Received: 2 September 2011 / Accepted: 21 November 2011 / Published online: 13 December 2011

Abstract The metabolic degradation of aldehydes is catalyzed by oxidoreductases from which aldehyde dehydrogenases (EC 1.2.1) comprise nonspecific or substrate-specific enzymes. The latter subset is represented, e.g., by NAD^+-dependent aminoaldehyde dehydrogenases (AMADHs; EC 1.2.1.19) oxidizing a group of naturally occurring ω-aminoaldehydes including polyamine oxidation products. Recombinant isoenzymes from pea (PsAMADH1 and 2) and tomato (LeAMADH1 and 2) were subjected to kinetic measurements with synthetic aldehydes containing a nitrogenous heterocycle such as pyridinecarbaldehydes and their halogenated derivatives, (pyridinylmethylamino)-aldehydes, pyridinyl propanals and aldehydes derived from purine, 7-deazapurine and pyrimidine to characterize their substrate specificity and significance of the resulting data for in vivo reactions. The enzymatic production of the corresponding carboxylic acids was analyzed by liquid chromatography coupled to electrospray ionization mass spectrometry. Although the studied AMADHs are largely homologous and supposed to have a very similar active site architecture, significant differences were observed. LeAMADH1 displayed the broadest specificity oxidizing almost all compounds followed by PsAMADH2 and 1. In contrast, LeAMADH2 accepted only a few compounds as substrates. Pyridinyl propanals were converted by all isoenzymes, usually better than pyridinecarbaldehydes and aldehydes with fused rings. The K_m values for the best substrates were in the range of 10^{-5}–10^{-4} M. Nevertheless, the catalytic efficiency values (V_{max}/K_m) reached only a very small fraction of that with 3-aminopropanal (except for LeAMADH1 activity with two pyridine-derived compounds). Docking experiments using the crystal structure of PsAMADH2 were involved to discuss differences in results with position isomers or alkyl chain homologs.

Keywords Aldehyde · Aminoaldehyde dehydrogenase · 7-Deazapurine · Pyridine · Pyrimidine · Purine

Abbreviations

AMADH	Aminoaldehyde dehydrogenase
AEAL	2-Aminoethanal
ABAL	4-Aminobutanal
ALDH	Aldehyde dehydrogenase
APAL	3-Aminopropanal
BADH	Betaine aldehyde dehydrogenase
LeAMADH	Tomato (*Lycopersicon esculentum*) aminoaldehyde dehydrogenase

Chemical names of all synthetic aldehyde compounds are abbreviated by acronyms (elucidated directly in the text) ending with a suffix AL.

Electronic supplementary material The online version of this article (doi:10.1007/s00726-011-1174-x) contains supplementary material, which is available to authorized users.

J. Frömmel · M. Tylichová · D. Kopečný · M. Šebela (✉)
Department of Protein Biochemistry and Proteomics, Centre of the Region Haná for Biotechnological and Agricultural Research, Faculty of Science, Palacký University, Šlechtitelů 11, 783 71 Olomouc, Czech Republic
e-mail: marek.sebela@upol.cz

M. Soural (✉)
Department of Organic Chemistry, Faculty of Science, Palacký University, 17. listopadu 12, 771 46 Olomouc, Czech Republic
e-mail: souralm@seznam.cz

G. Demo · M. Wimmerová
Central European Institute of Technology and Department of Biochemistry, Faculty of Science, Masaryk University, Kamenice 5, 625 00 Brno, Czech Republic

LC–MS	Liquid chromatography coupled to mass spectrometry
PsAMADH	Pea (*Pisum sativum*) aminoaldehyde dehydrogenase

Introduction

Aldehydes are highly reactive organic compounds. There are three groups of enzymes that catalyze their metabolic oxidation to the corresponding carboxylic acids: aldehyde dehydrogenases (ALDHs), aldehyde oxidases and xanthine oxidases (Panoutsopoulos et al. 2004; Marchitti et al. 2009). Currently, the protein superfamily of ALDHs consists of 24 families, from which for example plant enzymes are represented in 12 families (Kirch et al. 2004; Wood and Duff 2009). As expected, ALDH genes are found in virtually all genomes analyzed to date, indicating the biological significance of these enzymes (Vasiliou and Nebert 2005). Members of the ALDH superfamily catalyze the oxidation of numerous aldehyde substrates (Sophos and Vasiliou 2003) and use NAD^+ or $NADP^+$ as electron acceptors. ALDHs were originally shown to cluster into two main trunks of the phylogenetic tree (Perozich et al. 1999). The "class 1/2" trunk covers mostly nonspecific ALDHs including those from ALDH1 (cytosolic) and ALDH2 (mitochondrial) families classified under EC number 1.2.1.3. The second trunk ("class 3") contains substrate-specific ALDHs such as benzaldehyde dehydrogenase (EC 1.2.1.7), betaine aldehyde dehydrogenase (BADH, EC 1.2.1.8), nonphosphorylating glyceraldehyde 3-phosphate dehydrogenase (EC 1.2.1.9), aminoaldehyde dehydrogenase (AMADH, EC 1.2.1.19) and antiquitin (turgor-responsive ALDH, EC 1.2.1.31) (Perozich et al. 1999).

Nonspecific ALDHs (EC 1.2.1.3) convert aliphatic, alicyclic and aromatic aldehydes (Hill and Dickinson 1988; Klyosov 1996). Human mitochondrial ALDH2 is involved in the second step of ethanol metabolism (Farrés et al. 1994). Accordingly, ethanal and propanal represent its efficient substrates. On the other hand, ethanal can hardly function as the natural substrate for human cytosolic ALDH1, since its K_m far exceeds physiological concentrations (Klyosov 1996). An increase in aliphatic aldehyde chain length (up to C10) substantially decreases the K_m values of human ALDH2 and ALDH1 (Klyosov 1996). Interestingly, a recombinant ALDH2 from the plant *Craterostigma plantagineum* showed highest activity with nonanal (Kirch et al. 2001). Aromatic aldehydes (benzaldehydes, cinnamaldehydes, etc.) and fused polycyclic aldehydes, as well as derivatives of coumarin, quinoline, indole, and pyridine were recognized as tight-binding slow-turnover substrates for human ALDH2. Surprisingly, many of these aromatic compounds weakly inhibit ALDH1 (Klyosov 1996).

Benzaldehyde is also oxidized by a human member of the cytosolic ALDH3 family (Marchitti et al. 2007). It has been postulated that ALDH7 gene products are involved in adaptive metabolic pathways (Kirch et al. 2004). The human enzyme of this family is expressed in multiple cellular compartments, where it seems to mediate a protective role by generating osmolytes (Brocker et al. 2010). In this way, glycine betaine is formed from betaine aldehyde, which is otherwise known as a typical substrate of BADHs from the ALDH9 family (Chern and Pietruszko 1995). The ability to synthesize and/or accumulate glycine betaine is a ubiquitous adaptation to osmotic stress (Kirch et al. 2004). In mammals, ALDH7 is known to play a primary role in the pipecolic acid pathway of lysine catabolism catalyzing the oxidative conversion of aminoadipate semialdehyde to α-aminoadipic acid. Interestingly, human ALDH7 is able to oxidize benzaldehyde with a catalytic efficiency of 15% when compared with that for aminoadipate semialdehyde (Brocker et al. 2010).

Pea seedling aminoaldehyde dehydrogenase isoenzymes 1 and 2 (PsAMADH1 and 2), which belong to the ALDH9 family (according to the novel system by Kirch et al. 2004, the plant enzymes of this group should be classified within the ALDH10 family as well as BADHs), have been shown to oxidize pyridinecarbaldehydes (PCALs) as less efficient but still good substrates (Tylichová et al. 2010). Nevertheless, the isoenzymes prefer 3-aminopropanal (APAL), 4-aminobutanal (ABAL) and some other ω-aminoaldehydes as the best substrates indicating a relationship with polyamine metabolism (Šebela et al. 2000; Tylichová et al. 2010). In this work, PsAMADH1 and PsAMADH2 together with their counterparts from tomato (LeAMADH1 and 2) were subjected to an extensive study with synthetic nitrogenous heterocyclic aldehydes including derivatives of pyridine, purine, 7-deazapurine, pyrimidine plus several other compounds. Significant substrate specificity differences were observed among the studied enzymes. With the exception of LeAMADH2 that accepts only a few aromatic aldehydes as substrates, PsAMADH1 and 2 demonstrated much broader specificity. LeAMADH1 was found to be efficient with the heterocyclic aldehydes.

Materials and methods

Enzymes

Recombinant PsAMADH1 and PsAMADH2 were prepared as described previously (Tylichová et al. 2008, 2010). To obtain recombinant AMADH isoenzymes from tomato, the

total RNA from apical meristems and leaves of 7-day-old tomato seedlings (*Lycopersicon esculentum* cv. Amateur) was extracted using a Midi spin columns kit (Macherey-Nagel, Düren, Germany). Then the corresponding cDNA was synthesized using Superscript II reverse transcriptase (Invitrogen, Carlsbad, CA, USA). *LeAMADH1* ORF (1,515 bp; EMBL/GenBank accession no. AY796114) was amplified with synthetic oligonucleotides containing restriction sites—highlighted in bold—for BamHI (5′-CA G**GGATCC**GGCAAATCGTAATGTACCA-3′; sense primer) and XhoI (5′-CGT**CTCGAG**CTAATTCTTTGAAG GTGACTTAT-3′; antisense primer). *LeAMADH2* ORF (1,518 bp; EMBL/GenBank accession no. FJ228482) was amplified using another set of oligonucleotides containing either EcoRI restriction site (5′-CAT**GAATTC**GGCGA TTCCTAATATACGGAT-3′; sense primer), or KpnI restriction site (5′-AGT**GGTACC**TTACAGCTTTGAAG GAGACT-3′; antisense primer). Expression, cell lysis and enzyme purification were performed as described for PsAMADH1 (Tylichová et al. 2008). According to the actual needs, there was an additional purification step involving ion-exchange chromatography on a Resource Q column (GE Healthcare, Uppsala, Sweden) (Tylichová et al. 2010). Protein identification was done by peptide mass fingerprinting on a Microflex LRF20 MALDI-TOF mass spectrometer (Bruker Daltonik, Bremen, Germany) after SDS-PAGE and tryptic in-gel digestion (Šebela et al. 2006).

Commercial chemicals

Common chemicals and solvents were purchased from Sigma-Aldrich Chemie (Steinheim, Germany) as well as starting compounds for chemical syntheses, 3-(methylthio)propanal (Met-S-PAL), 3-(methylthio)butanal and 3-(5-methyl-2-furyl)butanal. The same company provided 2-, 3-and 4-bromobenzaldehyde (2-, 3-, 4-Br-BzAL); 2-, 3- and 4-pyridinecarbaldehyde (2-, 3-, 4-PCAL); 4-pyridinecarbaldehyde N-oxide (4-PCALNO); 2,6-dichloro-4-pyridinecarbaldehyde (2,6-diCl-4-PCAL); 3,5-dichloro-4-pyridinecarbaldehyde (3,5-diCl-4-PCAL); 2-bromo-4-pyridinecarbaldehyde (2-Br-4-PCAL) and 3-bromo-4-pyridinecarbaldehyde (3-Br-4-PCAL). (2-Pyridinylmethylamino)ethanal diethylacetal (2-PMet-AEAL diethylacetal), cat. no. S414859, and (4-pyridinylmethylamino)ethanal diethylacetal (4-PMet-AEAL diethylacetal), cat. no. S364746, were from Sigma-Aldrich Rare Chemical Library.

Preparation of synthetic compounds

Analytical data to all of the following synthetic compounds are provided in Supplementary material.

3-(Pyridinyl)-propanals

3-Pyridin-2-yl-propanal (P2PAL), 3-pyridin-3-yl-propanal (P3PAL) and 3-pyridin-4-yl-propanal (P4PAL) were synthesized according to a published procedure (Mancuso et al. 1978).

N-(2,2-dimethoxyethyl)-9H-purin-6-amine (Pu-AEAL dimethylacetal), N-(3,3-diethoxypropyl)-9H-purin-6-amine (Pu-APAL diethylacetal) and N-(4,4-diethoxybutyl)-9H-purin-6-amine (Pu-ABAL diethylacetal)

These compounds represent acetals of (9*H*-purin-6-ylamino)-aldehydes, i.e., purine derivatives of 2-aminoethanal (AEAL), APAL and ABAL. 6-Chloro-9*H*-purine (229 mg, 1.49 mmol) was dissolved in *n*-butanol (3 ml) and the corresponding dialkoxy-*n*-alkane-amine (3.0 mmol) was added. The reaction mixture was refluxed for 1 h (Pu-AEAL dimethylacetal), 4 h (Pu-APAL diethylacetal) or 9 h (Pu-ABAL diethylacetal), then evaporated to dryness and ice-cold water (10 ml) was added. The precipitated material was collected by suction, washed with ice-cold water and dried.

N-(2,2-dimethoxyethyl)-7H-pyrrolo[2,3-d]pyrimidin-4-amine (PyrPm-AEAL dimethylacetal), N-(3,3-diethoxypropyl)-7H-pyrrolo[2,3-d]pyrimidin-4-amine (PyrPm-APAL diethylacetal) and N-(4,4-diethoxybutyl)-7H-pyrrolo[2,3-d]pyrimidin-4-amine (PyrPm-ABAL diethylacetal)

These compounds represent acetals of (7*H*-pyrrolo[2,3-*d*]pyrimidin-4-yl)-aldehydes, i.e., 7-deazapurine derivatives of AEAL, APAL and ABAL. 4-Chloro-7*H*-pyrrolo[2,3-*d*]pyrimidine (114 mg, 0.75 mmol) was dissolved in ethanol (3 ml) and the corresponding dialkoxy-*n*-alkane-amine (1.5 mmol) was added. The reaction mixture was refluxed for 6 days (PyrPm-AEAL dimethylacetal) or 2 days (PyrPm-APAL and PyrPm-ABAL diethylacetals), then evaporated to dryness and the resulting residue was purified using column chromatography (DAVISIL LC60A 40–60 µm, toluene:acetonitrile:methanol 5:2:1).

N-(2,2-dimethoxyethyl)pyrimidin-2-amine (Pm-AEAL dimethylacetal), N-(3,3-diethoxypropyl)pyrimidin-2-amine (Pm-APAL diethylacetal) and N-(4,4-diethoxybutyl)pyrimidin-2-amine (Pm-ABAL diethylacetal)

These compounds represent acetals of (pyrimidin-2-ylamino)-aldehydes—pyrimidine derivatives of AEAL, APAL and ABAL. 2-Chloropyrimidine (114 mg, 1 mmol) was dissolved in *n*-butanol (2 ml) and the corresponding dialkoxy-*n*-alkane-amine (2.0 mmol) was added. The reaction mixture was refluxed for 3 h (Pm-AEAL

dimethylacetal) or 2 h (Pm-APAL and Pm-ABAL diethylacetals), then evaporated to dryness and the resulting residue was purified using column chromatography (DAVISIL LC60A 40–60 μm, toluene:acetonitrile 5:2).

Acetals of (pyridinylmethylamino)-aldehydes

The synthesis utilized a route adapted from the literature (Sánchez-Sandoval et al. 2003). For example, diethylacetal of 3-[(pyridin-2-ylmethyl)amino]propanal (2-PMet-APAL diethylacetal) was synthesized as follows: 3,3-diethoxypropane-1-amine (25 mmol) was dissolved in ethanol (25 ml). 2-Pyridinecarbaldehyde (26.5 mmol) was added dropwise to the solution and the resulting mixture was refluxed for 3 h. After cooling to laboratory temperature, $NaBH_4$ (35 mmol) was slowly added in small portions and then the mixture was stirred for 16 h. Then distilled water (50 ml) was added and the resulting solution was extracted with CH_2Cl_2 (3 × 50 ml). The combined organic layers were dried (Na_2SO_4). A yellow liquid product was obtained after evaporation of the solvent under reduced pressure in a yield of 88%. Acetals of the other (pyridinylmethylamino)-aldehydes were prepared by analogous procedures using the corresponding dialkoxy-*n*-alkane-amines and pyridinecarbaldehydes as starting compounds.

Instrumental analyses

LC–MS analyses of synthetic aldehyde compounds and reaction mixtures (after enzymatic oxidation of selected substrates) were carried out on a UHPLC chromatograph Accela equipped with a photodiode array detector and connected to a triple quadrupole mass spectrometer TSQ Quantum Access (both Thermo Scientific, CA, USA). A Nucleodur® C18 Gravity column (1.8 μm, 2.1 × 50 mm) was used at a flow rate of 0.8 ml min^{-1} and thermostated at 30°C (Macherey-Nagel). Mobile phases were as follows: (A) 10 mM ammonium acetate in water; (B) acetonitrile. There was a linear gradient from 10 to 80% B in 2.5 min, and then an isocratic run for 1.5 min. The column was re-equilibrated with 10% of B for 1 min. The APCI source operated at a discharge current of 5 μA, a vaporizer temperature of 400°C and a capillary temperature of 200°C. ^{1}H- and ^{13}C-NMR spectra were obtained on a Varian Unity*Plus* (299.89 MHz, ^{1}H) instrument. Measurements were performed at 21°C in DMSO-d_6 or chloroform-*d* solutions and referenced to the resonance signal of dimethylsulfoxide or chloroform.

Activity assay, kinetic measurements, protein assay

Enzyme activity was measured spectrophotometrically by monitoring the formation of NADH (ε_{340} = 6,620 M^{-1} cm^{-1}) at 23°C (Tylichová et al. 2010). The reaction mixture in a cuvette contained 0.15 M Tris–HCl buffer, pH 9.0, 0.5 mM NAD^+ and an appropriate amount of AMADH. For measurements of relative oxidation rate, the enzyme reaction was initiated by the addition of APAL (or another aldehyde) at a final concentration of 1 mM (Tylichová et al. 2010); for K_m and V_{max} determinations, substrate concentration varied according to needs. Acetals were converted to aldehydes by adding calculated amount of 0.4 M HCl just prior to measurements. Absorbance values were averaged from three independent experiments. Kinetic data were evaluated using GraphPad Prism 5.0 software. Proteins were determined by Bradford method (Bradford 1976) and, for the purified enzymes, using the following extinction coefficients calculated from the respective monomer amino acid sequences by ProtParam tool (http://www.expasy.org/tools/protparam.html): PsAMADH1 (ε_{280} = 82,390 M^{-1} cm^{-1}), PsAMADH2 (ε_{280} = 90,410 M^{-1} cm^{-1}), LeAMADH1 (ε_{280} = 75,860 M^{-1} cm^{-1}) and LeAMADH2 (ε_{280} = 94,880 M^{-1} cm^{-1}).

Docking experiments

The AutoDock 3.0 suite (Morris et al. 1998) was used as a molecular-docking tool. Semi-flexible protocols were followed, in which the target protein (PsAMADH2; PDB code: 3IWJ) was kept rigid. In contrast, aldehyde ligands being docked were kept flexible. The graphical user interface software Triton (Prokop et al. 2008) was employed to prepare, run, and analyze the docking simulations. Hydrogen atoms were added by WHAT IF (Vriend 1990). For partial atoms charges in the enzyme, the Kollman united atom charges were used (Weiner et al. 1984).

All ligands were built in Avogadro 1.0.0 (http://avogadro.openmolecules.net/). The geometries of the ligand structures were optimized using the Hartree–Fock method with a 6−31G(d) basis set as implemented in the Gaussian 03 program (Frisch et al. 2004). The electro-static potential fitting (ESP) charges were calculated, and the RESP procedure of the Antechamber program from the AMBER suite was used to generate input files for docking programs (Case et al. 2005; Pearlman et al. 1995). The rigid roots of each ligand were picked manually, in all cases the heterocyclic nitrogen atom was set as a rigid center. To get more useful results, the aldehyde bond in halogenated PCALs was made nonrotatable. All rotatable dihedrals in other ligands were allowed to rotate freely.

Grid maps were calculated by AutoGrid 3.0. from the AutoDock 3.0 suite. The grid box (60 × 60 × 60 Å) was centered to the substrate channel; grid point spacing was 0.375 Å. Docking calculations were carried out using Lamarckian genetic algorithm and a maximum of 100 conformers was considered for each compound. The population size was set to 50 and the individuals were

initialized randomly. The maximum number of energy evaluations was 5×10^6 and the maximum number of generations was 27,000. One top individual was allowed to survive the next generation and the mutation and crossover rates were set to 0.02 and 0.8, respectively. Step sizes were 2 Å for translations, 50° for quaternions and 50° for torsions. Cluster tolerance was 0.5 Å, external grid energy 1,000.0 and max initial energy 0.0.

Results and discussion

Motivation to this study

This work deals with design, preparation and testing of new synthetic substrates of plant AMADHs. The enzymes belong to the superfamily of ALDHs where individual dimeric or tetrameric proteins share a common overall folding pattern: each monomeric unit of 50–60 kDa comprises a substrate-binding (catalytic) domain, a coenzyme-binding domain and an oligomerization domain (Gruez et al. 2004; Tylichová et al. 2010). The active site of plant AMADHs, which is located between the coenzyme-binding and catalytic domains, is accessible via a wide (5–8 Å) and deep (15 Å) funnel passage allowing structurally diverse aldehydes to penetrate down to the catalytic cysteine and bind at this place for the possible catalytic conversion (Tylichová et al. 2010). That is why an idea came to mind to study synthetic compounds with heterocyclic nitrogen atom(s) and an aldehyde group, attached directly at the heterocycle or situated in a side chain, as potential substrates. The original motivation stemmed from the observation that PCALs are oxidized by PsAMADHs (Tylichová et al. 2010). It is worth mentioning that PCALs display a structural motif where the nitrogen atom is positioned toward the aldehyde group at a distance resembling that in natural ω-aminoaldehyde substrates. The oxidation of 2-, 3- and 4-PCAL by AMADH results in picolinic, nicotinic and isonicotinic acid, respectively. These are known as building blocks of more complex structures, for example tobacco alkaloids, compatible osmolytes and others (Kaiser et al. 1996; Rhodes and Hanson 1993). It has been also shown that exogenous 3-PCAL is metabolized to NAD^+ in mouse (Kaplan et al. 1957). Thus, through the action on nitrogenous heterocyclic aldehydes, AMADHs might participate in various biosynthetic routes.

Experimental setup

Based on their structural features, the studied synthetic compounds can be divided into a few groups. A majority of them include a pyridine ring: pyridinecarbaldehydes, 3-(pyridinyl)propanals, (pyridinylmethylamino)-aldehydes, and halogenderivates of pyridinecarbaldehydes. The other aldehyde compounds were derivatives of purine, 7-deazapurine or pyrimidine. Finally we also tested several aldehydes without heterocyclic nitrogen—methylthioaldehydes and a methylfurylaldehyde, which formally resemble natural ω-aminoaldehyde substrates of plant AMADHs. Chemical formulas of selected substances and the corresponding abbreviations are shown in Figs. 1 and 2.

3-(Pyridinyl)propanals were synthesized from 3-(pyridinyl)propanols using the Swern reaction with oxalyl chloride, dimethyl sulfoxide and triethylamine (Mancuso et al. 1978). Acetals of purine-, 7-deazapurine- and pyrimidine-derived aldehydes were obtained by a standard nucleophilic substitution: 6-chloropurine, 6-chloro-7-deazapurine, and 2-chloropyrimidine, respectively, were reacted with dialkoxy-*n*-alkane-amines (acetals of C2–C4 ω-aminoaldehydes) of desired length. Finally, acetals of (pyridinylmethylamino)-aldehydes were synthesized by a reductive amination from pyridinecarbaldehydes and acetals of C2–C4 ω-aminoaldehydes. All synthetic compounds were checked for purity (Supplementary material) by instrumental analysis prior to their testing in enzymatic reactions. The experimental set of plant AMADHs consisted of pea isoenzymes (PsAMADH1 and 2) and tomato isoenzymes (LeAMADH1 and 2). Biochemical properties

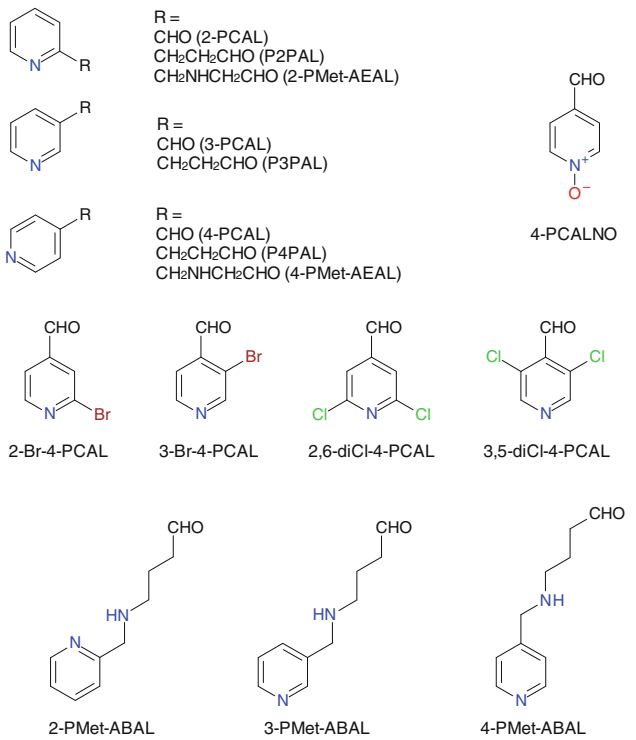

Fig. 1 Nitrogeneous heterocyclic aldehydes I. Chemical formulas of the studied pyridine-derived aldehydes were drawn using Accelrys Draw 4.0

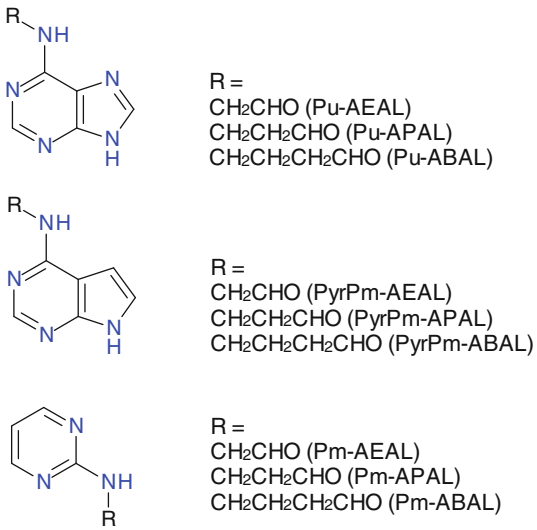

Fig. 2 Nitrogenous heterocyclic aldehydes II. Chemical formulas of the studied purine-, 7-deazapurine- and pyrimidine-derived aldehydes were drawn using Accelrys Draw 4.0

of pea AMADHs have already been reported in detail (Tylichová et al. 2010). LeAMADH1 and 2 were obtained by recombinant expression in a parallel project (details on their biochemical characterization will be published elsewhere). Kinetic analysis of the tomato enzymes with natural substrates indicated a significant difference in substrate specificity, when LeAMADH2, contrary to LeAMADH1, preferred markedly APAL to ABAL as the best substrate (Kopečný et al. unpublished results).

Evaluation of substrate properties of the synthetic compounds

First attempts to demonstrate substrate properties of the synthetic compounds relied on measurements of relative reaction rates at an expected saturating concentration of 1 mM in the reaction mixture. PCALs and PCALNO were oxidized by PsAMADHs only moderately and no consumption of the compounds was observed with LeAMADH2. On the other hand, they were found as very good substrates of LeAMADH1 with relative rate values between 28 and 84% of that with APAL as the best natural substrate (Table 1). 4-PCAL derivatives with 2- and 2,6-halogen substitution served as good substrates, while 4-PCAL derivatives with 3- or 3,5-halogen substituents were not oxidized at all. The measured relative rates were higher for the conversion by PsAMADH1 and LeAMADH1 than for the reactions of PsAMADH2 and LeAMADH2. All three3-(pyridinyl)propanals, higher homologs of PCALs resembling natural ω-aminoaldehydes by their

Table 1 Substrate specificity of PsAMADHs and LeAMADHs toward pyridine-derived aldehydes

Substrate	Relative reaction rate (%)			
	PsAMADH1	PsAMADH2	LeAMADH1	LeAMADH2
Pyridinecarbaldehydes				
2-PCAL	1	2	28	–
3-PCAL	1	4	84	–
4-PCAL	3	2	73	–
4-PCALNO	–	1	41	–
3-Br-4-PCAL	–	–	–	–
3,5-diCl-4-PCAL	–	–	–	–
2-Br-4-PCAL	28	3	60	2
2,6-diCl-4-PCAL	52	12	40	6
3-(Pyridinyl)propanals[a]				
P2PAL	3	35	52	4
P3PAL	26	11	127	4
P4PAL	25	34	91	19
(Pyridinylmethylamino)-aldehydes				
2-PMet-AEAL	–	–	–	–
4-PMet-AEAL	–	2	50	–
2-PMet-APAL	–	–	12	–
3-PMet-APAL	–	–	10	–
4-PMet-APAL	–	–	16	–
2-PMet-ABAL	29	25	88	38
3-PMet-ABAL	27	25	89	14
4-PMet-ABAL	25	29	85	15

Activities with substrates at 1 mM final concentration were measured in 0.15 M Tris–HCl buffer, pH 9.0, at 23°C. NAD^+ concentration in the reaction mixture was 0.5 mM. The rate of APAL oxidation was arbitrarily taken as 100%. The symbol "–" indicates no substrate properties

The relative reaction rates toward APAL conversion appear in the range of 1–3%

[a] Propanal itself represents a weak substrate of PsAMADHs (Tylichová et al. 2010) and LeAMADHs

aliphatic chain and the presence of positively charged nitrogen atom, were found very good substrates. The highest relative rates of their oxidation were observed with LeAMADH1. Using this enzyme, the relative reaction rate with P3PAL was surprisingly higher than with APAL itself.

2-PMet-AEAL was not oxidized at all, but its isomer 4-PMet-AEAL was converted by PsAMADH2 and particularly by LeAMADH1. All three position isomers of PMet-ABAL were oxidized well by all involved isoenzymes whereas PMet-APALs were converted only by LeAMADH1 at relative rates of 10–20% toward APAL oxidation (Table 1).

(9*H*-Purin-6-ylamino)-aldehydes (Pu-AEAL, Pu-APAL and Pu-ABAL) as well as (7*H*-pyrrolo[2,3-d]pyrimidin-4-ylamino)-aldehydes (PyrPm-AEAL, PyrPm-APAL and PyrPm-ABAL) exhibited diverse substrate properties (Table 2). LeAMADH2 did not accept the bicyclic compounds as substrates with the exception of a weak oxidation of Pu-AEAL. In contrast, LeAMADH1 oxidized all purinyl and deazapurinyl aminoaldehydes as effective substrates, only the relative reaction rate for the oxidation of Pu-APAL was below 10% when compared with the oxidation of the natural substrate APAL (Table 2). PsAMADH1 and 2 showed only restricted substrate preferences toward the purine and deazapurine derivatives. They slowly oxidized Pu-AEAL and PyrPm-ABAL, PsAMADH1 additionally converted Pu-ABAL. LeAMADH1 oxidized two of the analyzed (pyrimidin-2-ylamino)-aldehydes, i.e., Pm-AEAL and Pm-APAL. PsAMADH1 and PsAMADH2 showed activity only in exceptional cases (Table 2). Interestingly, Pm-ABAL was not a substrate of the studied enzymes.

To get further clues to understanding differences in substrate specificity of plant AMADHs, we also evaluated substrate properties of aldehydes containing a thioether group or a heterocyclic oxygen atom as well as the possible conversion of bromobenzaldehydes (structural analogs of the halogenated pyridinecarbaldehydes). 3-(Methylthio)propanal, a sulfur-containing analog of the natural aminoaldehyde substrates, was found the best substrate from this miscellaneous collection. The highest relative rate (77%) was observed with LeAMADH1, the other isoenzymes provided relative reaction rate values between 10 and 26%. 3-(Methylthio)butanal was oxidized only negligibly by PsAMADH1 and LeAMADH1, 4-(5-methylfur-2-yl)butanal was not a substrate. From the three

Table 2 Substrate specificity of PsAMADHs and LeAMADHs toward aldehydes derived from purine, 7-deazapurine and pyrimidine and some other compounds

Substrate	Relative reaction rate (%)			
	PsAMADH1	PsAMADH2	LeAMADH1	LeAMADH2
(9*H*-Purin-6-ylamino)-aldehydes				
Pu-AEAL	7	6	30	2
Pu-APAL	–	–	4	–
Pu-ABAL	3	–	20	–
(7*H*-Pyrrolo[2,3-d]pyrimidin-4-ylamino)-aldehydes				
PyrPm-AEAL	–	–	10	–
PyrPm-APAL	–	–	23	–
PyrPm-ABAL	7	8	57	–
(Pyrimidin-2-ylamino)-aldehydes				
Pm-AEAL	–	3	10	–
Pm-APAL	2	–	7	–
Pm-ABAL	–	–	–	–
Bromobenzaldehydes[a]				
2-Br-BzAL	–	–	–	–
3-Br-BzAL	0.7	1.2	4	1
4-Br-BzAL	0.2	0.3	3	–
Methylthioaldehydes				
Met-S-PAL	26	19	77	10
Met-S-BAL	1	–	2	–

Activities with substrates at 1 mM final concentration were measured in 0.15 M Tris–HCl buffer, pH 9.0, at 23°C. NAD^+ concentration in the reaction mixture was 0.5 mM. The rate of APAL oxidation was arbitrarily taken as 100%. The symbol "–"indicates no substrate properties

[a] Benzaldehyde itself is not oxidized at all by PsAMADH isoenzymes (Tylichová et al. 2010). In the case of LeAMADH2, zero activity was measured as well. Only LeAMADH1 accepts benzaldehyde as a weak substrate (the relative reaction rate toward APAL conversion is 3.4%)

isomers of bromobenzaldehyde, 3-Br-BzAL and 4-Br-BzaL were only moderately oxidized by LeAMADH1 (Table 2).

Determination of kinetic parameters K_m and V_{max}

For those substrates which were oxidized with relative rates reaching several per cents of that with APAL as a natural reference substrate, the fundamental kinetic parameters K_m and V_{max} were determined. As LeAMADH2 oxidized only a limited amount of the studied compounds and PsAMADH1 resembled the observed substrate preference of PsAMADH2 in a majority of reactions, the kinetic parameters were determined especially with PsAMADH2 and LeAMADH1 (only some supplementary K_m and V_{max} data were measured with PsAMADH1 and LeAMADH2). In the case of LeAMADH1, the measured V_{max} values reached from 10 to 60% of that with APAL as a reference substrate with the exception of Br-BzALs (around 1%); for PsAMADH2 it was from 5 to 40% except for 3-Br-BzAL, a majority of PCALs and 4-PMet-AEAL (all around 1%); see Table 3.

As regards to pyridine-derived aldehydes, the observed K_m values of PsAMADH2 (usually <100 μM) were mostly lower than their counterparts measured with LeAMADH1, or comparable (Table 3). Interestingly, in the case of 3-PCAL, 4-PMet-AEAL and 4-PMet-ABAL, the measured K_m values were of about 0.7 Mm, i.e., higher than those of LeAMADH1 (0.2–0.4 mM). On the other hand, the K_m values of LeAMADH1 generally appeared on the level of 0.1 mM except for those referring to the oxidation of 4-PCAL (19 μM) and 2-Br-4-PCAL (69 μM). In the first case, the K_m value was lower than the corresponding result with PsAMADH2 (Table 4).

In the case of PsAMADH1, we obtained relatively low K_m values of about 20 μM for both 3-PCAL and 4-PCAL. The K_m and V_{max} values (in parentheses) of PsAMADH1 for 2,6-diCl-4-PCAL and 2-Br-4-PCAL were 87 μM (24 nmol s^{-1} mg^{-1}) and 12 μM (17 nmol s^{-1} mg^{-1}), respectively. It is worth mentioning that the ratio V_{max}/K_m for 2-Br-4-PCAL and PsAMADH1 resembled that for the natural substrate APAL. The K_m values of LeAMADH2 for PCALs were between 150 and 350 μM. For 2,6-diCl-4-PCAL and 2-Br-4-PCAL, lower values of 38 and 25 μM, respectively, were measured. The binding of the position isomers of PMet-ABAL to LeAMADH1 and PsAMADH2 was reflected in relatively high K_m values of 0.2–0.8 mM. A very low K_m value of 3.2 μM of LeAMADH1 was determined for the oxidation of 4-Br-BzAL (Table 4). In the case of the oxidation of bicyclic aldehydes by

Table 3 Kinetic parameters of PsAMADH2 and LeAMADH1 for the oxidation of pyridine-derived aldehydes

Substrate	PsAMADH2			LeAMADH1		
	K_m	V_{max}	V_{max}/K_m	K_m	V_{max}	V_{max}/K_m
Reference substrate						
APAL	12 ± 1.2	179 ± 5.1	1	20 ± 3.3	167 ± 12.2	1
Pyridinecarbaldehydes						
2-PCAL	77 ± 5.2	2.1 ± 0.03	0.002	187 ± 11.2	18 ± 0.4	0.012
3-PCAL	754 ± 32.4	7.8 ± 0.13	0.001	238 ± 21.6	52 ± 1.7	0.026
4-PCAL	33 ± 2.3	2.1 ± 0.04	0.004	19 ± 1.3	59 ± 1.2	0.372
4-PCALNO	55 ± 3.1	0.8 ± 0.01	0.001	356 ± 29.1	30 ± 0.9	0.010
2,6-diCl-4-PCAL	28 ± 0.5	15 ± 0.5	0.036	162 ± 14.8	36 ± 1.4	0.027
2-Br-4-PCAL	32 ± 1.7	3.6 ± 1.72	0.008	69 ± 7.1	65 ± 2.7	0.113
3-(Pyridinyl)propanals						
P2PAL	171 ± 10.9	42 ± 0.9	0.016	161 ± 12.2	33 ± 0.8	0.025
P3PAL	87 ± 8.0	22 ± 0.8	0.017	129 ± 7.1	94 ± 2.0	0.087
P4PAL	29 ± 2.1	70 ± 1.3	0.162	146 ± 9.2	68 ± 1.8	0.056
(Pyridinylmethylamino)-aldehydes						
4-PMet-AEAL	761 ± 59.4	3.4 ± 0.10	0.0003	238 ± 9.7	34 ± 0.5	0.017
2-PMet-ABAL	401 ± 38.9	25 ± 1.0	0.004	390 ± 30.4	52 ± 1.7	0.016
3-PMet-ABAL	289 ± 16.4	27 ± 0.6	0.006	294 ± 16.2	75 ± 1.6	0.031
4-PMet-ABAL	679 ± 69.3	40 ± 2.8	0.004	385 ± 28.9	44 ± 1.3	0.014

Activities were measured in 0.15 M Tris–HCl buffer, pH 9.0, at 23°C. A saturating NAD^+ concentration of 0.5 mM was used. K_m and V_{max} values (shown in μM and nmol s^{-1} mg^{-1}, respectively) were calculated from the Lineweaver–Burk and Eadie–Scatchard plots of initial rates as arithmetic means of values from both plots. V_{max}/K_m ratios are provided as relative values toward that for APAL, which was set arbitrarily equal to 1

Table 4 Kinetic parameters of PsAMADH2 and LeAMADH1 for the oxidation of some other substrates

Substrate	PsAMADH2			LeAMADH1		
	K_m	V_{max}	V_{max}/K_m	K_m	V_{max}	V_{max}/K_m
Reference substrate						
APAL	12 ± 1.2	179 ± 5.1	1	20 ± 3.3	167 ± 12.2	1
Bromobenzaldehydes						
3-Br-BzAL	13 ± 0.9	1.16 ± 0.020	0.006	69 ± 6.3	2.3 ± 0.07	0.004
4-Br-BzAL	ND	ND	ND	3.2 ± 0.18	1.3 ± 0.04	0.049
Purine- and 7-deazapurine-derived aldehydes						
Pu-AEAL	755 ± 55.2	9.6 ± 0.4	0.0009	379 ± 22.8	21 ± 0.5	0.007
Pu-ABAL	ND	ND	ND	482 ± 25.2	14 ± 0.3	0.004
PyrPm-APAL	ND	ND	ND	1,023 ± 68.9	24 ± 0.8	0.003
PyrPm-ABAL	ND	ND	ND	1,245 ± 92.1	65 ± 2.9	0.006
Methylthioaldehydes						
Met-S-PAL	44 ± 3.4	21 ± 0.4	0.032	29 ± 1.2	43 ± 0.4	0.178

Activities were measured in 0.15 M Tris–HCl buffer, pH 9.0, at 23°C. A saturating NAD^+ concentration of 0.5 mM was used. K_m and V_{max} values (shown in μM and nmol s^{-1} mg^{-1}, respectively) were calculated from the Lineweaver–Burk and Eadie–Scatchard plots of initial rates as arithmetic means of values from both plots. V_{max}/K_m ratios are provided as relative values toward that for APAL, which was set arbitrarily equal to 1. The abbreviation ND stands for "not determined" and refers to those cases, where activity was too low to measure the kinetic parameters

LeAMADH1, the K_m values were around 400 μM for purine-derived aldehydes and over 1 mM for 7-deazapurine-derived aldehydes. PsAMADH1 oxidized PyrPm-ABAL with a K_m value of 280 μM and PsAMADH2 oxidized Pu-AEAL providing a K_m value of 755 μM. 3-Methylthiopropanal was oxidized by all four studied AMADH isoenzymes providing K_m values between 10 and 50 μM. The highest value of 44 μM was determined for its oxidation by PsAMADH2, for LeAMADH1 the K_m value was 29 μM (Table 4). The V_{max}/K_m ratios presented in Tables 3 and 4 clearly show that only some pyridine-derived aldehydes can be considered good substrates of pea and tomato AMADHs. The other oxidized compounds should be referred to as weak substrates. Examples of V_{max} and K_m determination from the measured data are provided in Fig. 3.

Analysis of the reaction mixture by LC–MS

During oxidation of an ω-aminoaldehyde substrate in AMADH reaction, the release of the corresponding ω-amino acid is accompanied by the formation of NADH. There are two ways for analyzing the possible substrate properties of an aldehyde compound toward AMADH. In the above text, the described kinetic parameters were measured by monitoring the changes in NADH absorption at 340 nm (the well-known optical test for NAD^+-dependent dehydrogenases by Warburg and Christian 1943). The second possibility is based on a direct measurement of carboxylic acid in the reaction mixture, which appears as a product along with NADH. Due to its unparalleled speed, sensitivity, specificity and ease of use, mass spectrometry has emerged as a powerful tool for identifying organic compounds (Crews et al. 2010). Solutions of the studied aldehydes made in a mass-spectrometry compatible buffer (ammonium bicarbonate) were incubated with the enzyme and then subjected to ultrafiltration (10-kDa-cutoff Microcon centrifugation cartridges by Millipore, Bedford, MA, USA) for obtaining a protein-free filtrate. The filtrate was then separated by LC–MS (see "Materials and methods" for details). Pyridinecarboxylates were previously demonstrated as products in the individual reaction mixtures of PsAMADH2 and the three position isomers of pyridinecarbaldehydes. In that case, however, no separation was involved and the samples were directly introduced into the mass spectrometer (Tylichová et al. 2010). Figure 4 shows the LC–MS analysis of the reaction mixture of LeAMADH1 and Pu-ABAL. 4-(*9H*-Purin-6-ylamino)-butyric acid was eluted at 0.98 min (*m/z* 222 and *m/z* 204—neutral loss of water; $[M+H]^+$) in contrast to the aldehyde at 2.23 min (*m/z* 206, not shown; $[M+H]^+$). (Pyridinylmethyl)-aminobutyric acids (*m/z* 195 and *m/z* 177—neutral loss of water; $[M+H]^+$) were demonstrated as products of the enzymatic oxidation of PMet-ABALs. 2,6-diCl-4-PCAL was oxidized to 2,6-dichloroisonicotinic acid (*m/z* 193; $[M+H]^+$). Similarly, the expected oxidation products of Met-S-PAL, P3PAL, Pu-AEAL and PyrPm-ABAL were detected by peaks with *m/z* 121, 152, 194 and 221, respectively.

Docking of substrates into the active site of PsAMADH2

As there is the crystal structure of PsAMADH2 available (Tylichová et al. 2010), docking experiments were

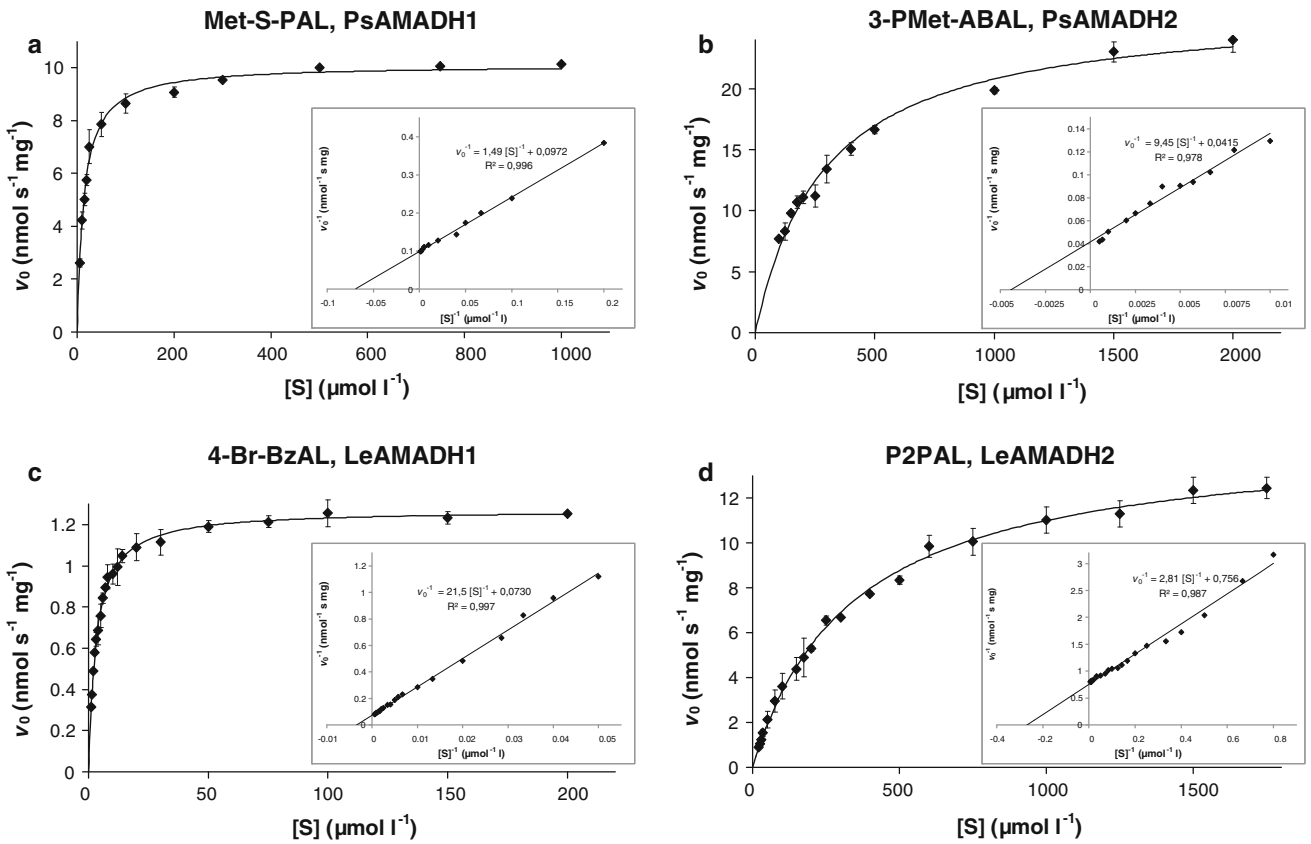

Fig. 3 Substrate properties of the studied compounds. There are selected saturation curves from kinetic measurements shown with the corresponding Lineveaver–Burk plots (in the *insets*); symbols on axes: v_o, initial velocity; [S], substrate concentration. Enzyme activity was assayed spectrophotometrically by monitoring the formation of NADH at 23°C. The reaction proceeded in 0.15 M Tris–HCl buffer, pH 9.0: **a** oxidation of 3-(methylthio)propanal (Met-S-PAL) by PsAMADH1; **b** oxidation of 4-[(pyridin-3-ylmethyl)amino]butanal (3-PMet-ABAL) by PsAMADH2; **c** oxidation of 4-bromobenzaldehyde (4-Br-BzAL) by LeAMADH1; **d** oxidation of 3-pyridin-2-yl-propanal (P2PAL) by LeAMADH2

involved to look closer at the interactions of PsAMADH2 and halogenated 4-pyridinecarbaldehydes or (pyridinylmethylamino)-aldehydes. The kinetic results obtained with these compounds revealed significant differences related to the position of the halogen substituent and the length and position of the aldehyde side chain, respectively, at the pyridine ring. Only 2- or 2,6-halogen derivatives of 4-PCAL were found substrates of the studied enzymes, whereas the corresponding 3- or 3,5-halogen derivatives were not oxidized at all. Figure 5 shows the docking results for 2,6-diCl-4-PCAL and 3,5-diCl-4-PCAL. The simulated binding provided a rotated position of the pyridine ring in 3,5-diCl-4-PCAL toward that of 2,6-diCl-4-PCAL. In consequence, the distance between the carbon atom in the ligand carbonyl group and Cys 294 sulfur increased from 3.6 Å in the case of 2,6-diCl-4-PCAL to 4.9 Å in the case of 3,5-diCl-4-PCAL. A comparison of the docking results for 4-PMet-ABAL, 2-PMet-ABAL, 4-PMet-APAL and 2-PMet-APAL indicated a similar binding simulation with the carbonyl group guided to the catalytic Cys294 of PsAMADH2 (Fig. 6). The distance between the carbon atom in the ligand carbonyl group and Cys 294 sulfur increased from 3.8 Å in the case of both PMet-ABALs to 5.0 and 5.1 Å in the case of 2-PMet-APAL and 4-PMet-APAL, respectively. The docking studies demonstrated that despite binding of a pyridine-derived aldehyde compound at the active site, substituents on the heterocycle and the length of the attached aliphatic chain carrying the aldehyde group may result in a binding mode which obstructs the productive interaction with the catalytic thiol.

Structural clues to substrate specificity of plant AMADHs have recently been investigated using site-directed mutagenesis (Kopečný et al. 2011). The enzymes possess a substrate channel with acidic amino acid residues at the entrance and aromatic amino acid residues in the interior (Tylichová et al. 2010). The acidic residues are essential for both the activity and affinity of the enzymes to ω-aminoaldehydes: PsAMADH2 turns into a nonspecific aldehyde dehydrogenase with capronaldehyde as the best substrate upon triple mutation E106A+D110A+D113A. The aromatic residues (Y163, W170 and W288 in PsAMADH2) contribute to an appropriate orientation of the

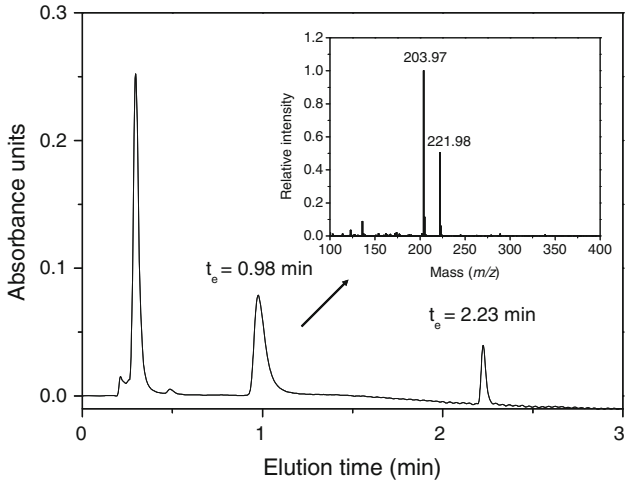

Fig. 4 LC–MS of the reaction mixture containing LeAMADH1 and 4-(9*H*-purin-6-ylamino)butanal (Pu-ABAL). The reaction mixture in a total volume of 2 ml contained 100 mM NH_4HCO_3, 1.5 mM NAD^+, 1 mM substrate and 100 µg of recombinant LeAMADH1. On mixing the components, it was incubated overnight at 23°C. *Main panel* liquid chromatographic separation of the reaction mixture on a Nucleodur® C18 Gravity column. *Inset* a mass spectrum of the fraction eluted in the retention time interval 0.95–1.07 min with two dominants peaks—*m/z* 222 refers to a pseudomolecular ion $[M+H]^+$ of 4-(9*H*-purin-6-ylamino)butyric acid, *m/z* 204 then indicates a neutral loss of water from the compound. The fraction eluted in the retention time interval 2.21–2.27 min provided a mass spectrum consistent with unreacted 4-(9*H*-purin-6-ylamino)butanal, i.e., Pu-ABAL (a pseudomolecular ion with *m/z* 206; not shown)

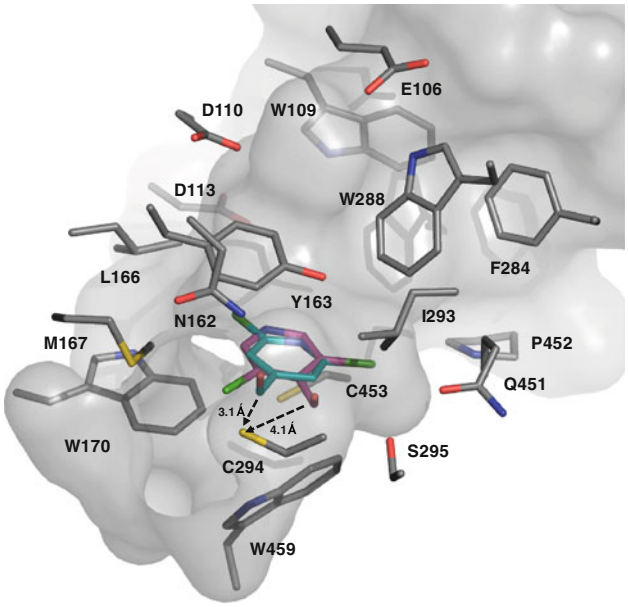

Fig. 5 Docking of dichloro-pyridinecarbaldehydes into the active site of PsAMADH2. The docked molecules of 2,6-dichloropyridine-4-pyridinecarbaldehyde (2,6-diCl-4-PCAL) and 3,5-dichloro-4-pyridinecarbaldehyde (3,5-diCl-4-PCAL) are superposed for comparison. Carbon atoms of 2,6-diCl-4-PCAL and 3,5-diCl-4-PCAL are colored in *turquoise blue* and *magenta*, respectively, oxygen atoms are in *red*, nitrogen atoms in *blue* and chlorine atoms in *green*. Active-site residues of PsAMADH2 (PDB: 3IWJ) are labeled and depicted in *atom-coded colors*. *Black arrows* indicate the calculated distance between the carbon atom in the ligand carbonyl group and sulfur atom of the catalytic C294, which is 3.6 and 4.9 Å for 2,6-diCl-4-PCAL and 3,5-diCl-4-PCAL, respectively. Substrate channel surface was calculated using Hollow (Ho and Gruswitz 2008). Docking was performed using Autodock 3.0 (Morris et al. 1998); structures were drawn by PyMOL 1.2 (DeLano 2002) (color figure online)

substrate toward the catalytic cysteine (Kopečný et al. 2011). The residue W109 in PsAMADH2, which divides the upper funnel-shaped domain of the substrate channel into two halves (Tylichová et al. 2010), is replaced by alanine in PsAMADH1 and LeAMADH1 and serine in LeAMADH2. Such a substitution does not influence kinetic properties as demonstrated by measurements with W109A mutant of PsAMADH2 (Kopečný et al. 2011). However, when it is accompanied by an additional substitution of W288 to A288 like in the case of LeAMADH1, the substrate channel becomes larger and thus more accessible for bulkier substrates (e.g., purine- and 7-deazapurine-derived aldehydes described in this study). The presence of F288 instead of W288 in PsAMADH1 increases the cavity diameter to a smaller extent. In consequence, the difference in substrate specificity between PsAMADH1 and PsAMADH2 is less pronounced than that between PsAMADH2 and LeAMADH1.

Conclusions

AMADHs have long been known as enzymes that oxidize ω-aminoaldehydes. However, recently published studies have shown that they appear to have rather broad substrate specificity including also aldehydes with *n*-alkyl chains as well as certain nitrogenous heterocyclic aldehydes (Gruez et al. 2004; Tylichová et al. 2010). We provide further evidence to support the knowledge of less-specific character of the enzymes. There are four main findings that result from the present study. Firstly, plant AMADHs are able to oxidize aldehydes derived from pyridine, purine, 7-deazapurine and pyrimidine. In addition, some halogenderivatives of pyridinecarbaldehydes are also converted. When compared with the conversion of aromatic and aromatic heterocyclic aldehydes by human mitochondrial ALDH2 (Klyosov 1996), their binding at the active site is much weaker as documented by the results of experimental determination of Michaelis constants. For example, the affinity of human ALDH2 to 3-PCAL is characterized by a K_m value of 2 µM, whereas PsAMADH2 and LeAMADH1 shows K_m values higher by one or two orders of magnitude. Based on the determined catalytic efficiency values, only a very few compounds from the studied collection can be considered good substrates. Secondly, due to their relatively high K_m values (in comparison with the

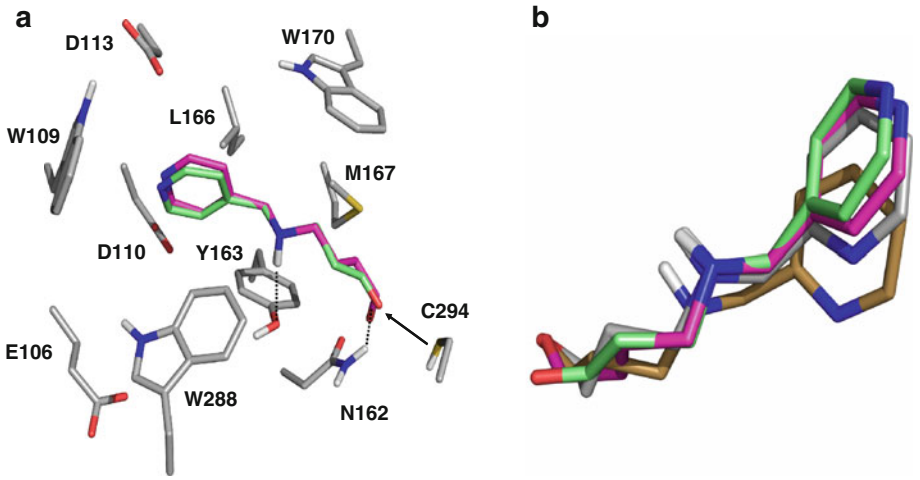

Fig. 6 Docking of (pyridinylmethylamino)-aldehydes into the active site of PsAMADH2. **a** Superposition of 4-[(pyridin-4-ylmethyl) amino]butanal (4-PMet-ABAL) and 3-[(pyridin-4-ylmethyl) amino]propanal (4-PMet-APAL) docked into the active site of PsAMADH2 (PDB: 3IWJ). Carbon atoms of 4-PMet-ABAL and 4-PMet-APAL are colored in *magenta* and *green*, respectively, oxygens are in *red*, nitrogens in *blue* and hydrogens in *light gray*. Active-site residues of PsAMADH2 are labeled and depicted in *atom-coded colors*. *Dashed lines* indicate possible hydrogen bonding interactions. The calculated distance between the carbon atom in the ligand carbonyl group and sulfur atom of the catalytic C294 (*black arrow*) is 3.8 and 5.1 Å for 4-PMet-ABAL and 4-PMet-APAL, respectively. **b** A superposition of the docked molecules (see from the top to the bottom with respect to the pyridine ring): 4-PMet-APAL (*green*), 4-PMet-ABAL (*magenta*), 2-PMet-ABAL (*gray*) and 2-PMet-APAL (*light brown*). Docking was performed using Autodock 3.0 (Morris et al. 1998); structures were drawn by PyMOL 1.2 (DeLano 2002) (color figure online)

physiological substrate APAL), nitrogenous heterocyclic compounds probably cannot represent substrates under in vivo conditions, nevertheless they might be efficiently converted at high concentration levels contributing in this way to the detoxifying role of AMADHs in the cell. Thirdly, substrate properties toward plant AMADHs of nitrogenous heterocyclic aldehydes are significantly dependent on the ring substitution pattern or the length of the aldehyde side chain. It has been described that *o*-benzaldehydes and 2-substituted naphthaldehydes are worse substrates of human ALDH2 than their isomers with a substitution at more distant positions toward the aldehyde group (Klyosov 1996). Similar observations were made also in this work, e.g., for 4-PCAL derivatives with halogen atom substitutions. Finally, we demonstrated that plant AMADH isoenzymes may show a big divergence with respect to their substrate specificity. This is not surprising for an interspecific comparison of AMADHs like in the case of pea and tomato but surprises at the level of a single species (e.g., LeAMADH1 vs. LeAMADH2). Such diversity might be helpful for selecting proper isoenzyme candidates applicable to organic synthesis or as a biorecognition element in analytical devices (e.g., biosensors for the determination of aminoaldehydes and aldehydes in food, drinks and other biological samples). In plant biotechnology, transgenic plants overexpressing aldehyde dehydrogenase genes are studied with the aim of improving stress tolerance by metabolizing toxic aldehydes (Sunkar et al. 2003).

Acknowledgments This work was supported by OP RD&I grant no. ED0007/01/01 (Centre of the Region Haná for Biotechnological and Agricultural Research) and grant no. MSM0021622413 from the Ministry of Education, Youth and Sports, Czech Republic, plus grant no. 522/08/0555 from the Czech Science Foundation. We would also like to thank Hana Moskalíková, a former student of the Department of Biochemistry, Faculty of Science, Palacký University, for her valuable contribution to initial experiments.

Conflict of interest The authors declare no conflict of interest.

References

Bradford MM (1976) A rapid and sensitive method for the quantitation of microgram quantities of protein utilizing the principle of protein-dye binding. Anal Biochem 72:248–254. doi:10.1016/0003-2697(76)90527-3

Brocker C, Lassen N, Estey T, Pappa A, Cantore M, Orlova VV, Chavakis T, Kavanagh KL, Oppermann U, Vasiliou V (2010) Aldehyde dehydrogenase 7A1 (ALDH7A1) is a novel enzyme involved in cellular defense against hyperosmotic stress. J Biol Chem 285:18452–18463. doi:10.1074/jbc.M109.077925

Case DA, Cheatham TE, Darden T, Gohlke H, Luo R, Merz KM, Onufriev A, Simmerling C, Wang B, Woods RJ (2005) The amber biomolecular simulation programs. J Comput Chem 26:1668–1688. doi:10.1002/jcc.20290

Chern MK, Pietruszko R (1995) Human aldehyde dehydrogenase E3 isozyme is a betaine aldehyde dehydrogenase. Biochem Biophys Res Commun 213:561–568. doi:10.1006/bbrc.1995.2168

Crews P, Rodríguez J, Jaspars M (2010) Organic structure analysis, 2nd edn. Oxford University Press, New York, p 273

DeLano W (2002) The PyMOL molecular graphics system. DeLano Scientific, Palo Alto. http://www.pymol.org

Farrés J, Wang X, Takahashi K, Cunningham SJ, Wang TT, Weiner H (1994) Effects of changing glutamate 487 to lysine in rat and human liver mitochondrial aldehyde dehydrogenase. A model to study human (oriental type) class 2 aldehyde dehydrogenase. J Biol Chem 269:13854–13860

Frisch MJ, Trucks GW, Schlegel HB, Scuseria GE, Robb MA, Cheeseman JR, Montgomery JA Jr, Vreven T, Kudin KN, Burant JC, Millam JM, Iyengar SS, Tomasi J, Barone V, Mennucci B, Cossi M, Scalmani G, Rega N, Petersson GA, Nakatsuji H, Hada M, Ehara M, Toyota K, Fukuda R, Hasegawa J, Ishida M, Nakajima T, Honda Y, Kitao O, Nakai H, Klene M, Li X, Knox JE, Hratchian HP, Cross JB, Bakken V, Adamo C, Jaramillo J, Gomperts R, Stratmann RE, Yazyev O, Austin AJ, Cammi R, Pomelli C, Ochterski JW, Ayala PY, Morokuma K, Voth GA, Salvador P, Dannenberg JJ, Zakrzewski VG, Dapprich S, Daniels AD, Strain MC, Farkas O, Malick DK, Rabuck AD, Raghavachari K, Foresman JB, Ortiz JV, Cui Q, Baboul AG, Clifford S, Cioslowski J, Stefanov BB, Liu G, Liashenko A, Piskorz P, Komaromi I, Martin RL, Fox DJ, Keith T, Al-Laham MA, Peng CY, Nanayakkara A, Challacombe M, Gill PMW, Johnson B, Chen W, Wong MW, Gonzalez C, Pople JA (2004) Gaussian 03, Revision C.02. Gaussian Inc., Wallingford

Gruez A, Roig-Zamboni V, Grisel S, Salomoni A, Valencia C, Campanacci V, Tegoni M, Cambillau C (2004) Crystal structure and kinetics identify *Escherichia coli* YdcW gene product as a medium-chain aldehyde dehydrogenase. J Mol Biol 343:29–41. doi:10.1016/j.jmb.2004.08.030

Hill JP, Dickinson FM (1988) Pre-steady-state kinetics of aldehyde oxidation by pig liver cytosolic aldehyde dehydrogenase. Biochem Soc Trans 16:856–857

Ho BK, Gruswitz F (2008) HOLLOW: generating accurate representations of channel and interior surfaces in molecular structures. BMC Struct Biol 8:49. doi:10.1186/1472-6807-8-49

Kaiser JP, Feng Y, Bollag JM (1996) Microbial metabolism of pyridine, quinoline, acridine, and their derivatives under aerobic and anaerobic conditions. Microbiol Rev 60:483–498

Kaplan NO, Goldin A, Humphreys SR, Stolzenbach FE (1957) Pyridine precursors of mouse liver diphosphopyridine nucleotide. J Biol Chem 226:365–371

Kirch HH, Nair A, Bartels D (2001) Novel ABA- and dehydration-inducible aldehyde dehydrogenase genes isolated from the resurrection plant *Craterostigma plantagineum* and *Arabidopsis thaliana*. Plant J 28:555–567. doi:10.1046/j.1365-313X.2001.01176.x

Kirch HH, Bartels D, Wei Y, Schnable PS, Wood AJ (2004) The ALDH gene superfamily of *Arabidopsis*. Trends Plant Sci 9:371–377. doi:10.1007/s11103-004-7796-6

Klyosov AA (1996) Kinetics and specificity of human liver aldehyde dehydrogenase toward aliphatic, aromatic, and fused polycyclic aldehydes. Biochemistry 35:4457–4467. doi:10.1021/bi9521102

Kopečný D, Tylichová M, Snégaroff J, Popelková H, Šebela M (2011) Carboxylate and aromatic active-site residues are determinants of high-affinity binding of ω-aminoaldehydes to plant aminoaldehyde dehydrogenases. FEBS J 278:3130–3139. doi:10.1111/j.1742-4658.2011.08239.x

Mancuso AJ, Huang SL, Swern D (1978) Oxidation of long-chain and related alcohols to carbonyls by dimethyl sulfoxide "activated" by oxalyl chloride. J Org Chem 43:2480–2482. doi:10.1021/jo00406a041

Marchitti SA, Orlicky DJ, Vasiliou V (2007) Expression and initial characterization of human ALDH3B1. Biochem Biophys Res Commun 356:792–798. doi:10.1016/j.bbrc.2007.03.046

Marchitti SA, Brocker C, Stagos D, Vasiliou V (2009) Non-P450 aldehyde oxidizing enzymes: the aldehyde dehydrogenase superfamily. Expert Opin Drug Metab Toxicol 4:697–720. doi:10.1517/17425250802102627

Morris GM, Goodsell DS, Halliday RS, Huey R, Hart WE, Belew RK, Olson AJ (1998) Automated docking using a Lamarckian genetic algorithm and an empirical binding free energy function. J Comput Chem 19:1639–1662. doi:10.1002/(SICI)1096-987X(19981115)19:14<1639:AID-JCC10>3.0.CO;2-B

Panoutsopoulos GI, Kouretas D, Beedham C (2004) Contribution of aldehyde oxidase, xanthine oxidase, and aldehyde dehydrogenase on the oxidation of aromatic aldehydes. Chem Res Toxicol 2004:1368–1376. doi:10.1021/tx030059u

Pearlman DA, Case DA, Caldwell JW, Ross WS, Cheatham TE, Debolt S, Ferguson D, Seibel G, Kollman P (1995) Amber, a package of computer programs for applying molecular mechanics, normal mode analysis, molecular dynamics and free energy calculations to simulate the structural and energetic properties of molecules. Comput Phys Commun 91:1–41. doi:10.1016/0010-4655(95)00041-D

Perozich J, Nicholas H, Wang BC, Lindahl R, Hempel J (1999) Relationships within the aldehyde dehydrogenase extended family. Protein Sci 8:137–146. doi:10.1110/ps.8.1.137

Prokop M, Adam J, Kříž Z, Wimmerová M, Koča J (2008) TRITON: a graphical tool for ligand-binding protein engineering. Bioinformatics 24:1955–1956. doi:10.1093/bioinformatics/btn344

Rhodes D, Hanson AD (1993) Quarternary ammonium and tertiary sulfonium compounds in higher plants. Annu Rev Plant Physiol Plant Mol Biol 44:357–384. doi:10.1146/annurev.pp.44.060193.002041

Sánchez-Sandoval A, Alvarez-Toledano C, Gutiérrez-Pérez Y, Reyes-Ortega Y (2003) A modified procedure for the preparation of linear polyamines. Synth Commun 33:481–492. doi:10.1081/SCC-120015780

Šebela M, Brauner F, Radová A, Jacobsen S, Havliš J, Galuszka P, Peč P (2000) Characterization of a homogenous plant aminoaldehyde dehydrogenase. Biochim Biophys Acta 1480:329–341. doi:10.1016/S0167-4838(00)00086-8

Šebela M, Štosová T, Havliš J, Wielsch N, Thomas H, Zdráhal Z, Shevchenko A (2006) Thermostable trypsin conjugates for high-throughput proteomics: synthesis and performance evaluation. Proteomics 6:2959–2963. doi:10.1002/pmic.200500576

Sophos NA, Vasiliou V (2003) Aldehyde dehydrogenase gene superfamily: the 2002 update. Chem Biol Interact 143–144:5–22. doi:10.1016/S0009-2797(02)00163-1

Sunkar R, Bartels D, Kirch HH (2003) Overexpression of a stress-inducible aldehyde dehydrogenase gene from *Arabidopsis thaliana* in transgenic plants improves stress tolerance. Plant J 35:452–464. doi:10.1046/j.1365-313X.2003.01819.x

Tylichová M, Briozzo P, Kopečný D, Ferrero J, Moréra S, Joly N, Snégaroff J, Šebela M (2008) Purification, crystallization and preliminary crystallographic study of a recombinant plant aminoaldehyde dehydrogenase from *Pisum sativum*. Acta Crystallogr Sect F Struct Biol Cryst Commun 64:88–90. doi:10.1107/S1744309107068522

Tylichová M, Kopečný D, Moréra S, Briozzo P, Lenobel R, Snégaroff J, Šebela M (2010) Structural and functional characterization of plant aminoaldehyde dehydrogenase from *Pisum sativum* with a broad specificity for natural and synthetic aminoaldehydes. J Mol Biol 396:870–882. doi:10.1016/j.jmb.2009.12.015

Vasiliou V, Nebert DW (2005) Analysis and update of the human aldehyde dehydrogenase (ALDH) gene family. Hum Genomics 2:138–143

Vriend G (1990) WHAT IF—a molecular modeling and drug design program. J Mol Graph 8:52–56

Warburg O, Christian W (1943) Isolierung und Kristallisation des Gärungsferments Zymohexase. Biochem Z 314:149–176 (in German)

Weiner SJ, Kollman PA, Case DA, Singh UC, Ghio C, Alagona G, Profeta S, Weiner P (1984) A new force-field for molecular mechanical simulation of nucleic acids and proteins. J Am Chem Soc 106:765–784. doi:10.1021/ja00315a051

Wood AJ, Duff RJ (2009) The aldehyde dehydrogenase (ALDH) gene superfamily of the moss *Physcomitrella patens* and the algae *Chlamydomonas reinhardtii* and *Ostreococcus tauri*. Bryologist 112:1–11. doi:10.1639/0007-2745-112.1.1